ELSEVIER

Finite Elements in Analysis and Design 28 (1998) 293–302

FINITE ELEMENTS IN ANALYSIS AND DESIGN

Finite element analysis of pressure vessel using beam on elastic foundation analysis

Fuang-Yuan Huang*, Gao-Liang Shi

Department of Mechanical Engineering, National Central University, Chung-Li, Taiwan

Abstract

In this study, we first applied the variation principle to derive a new finite element method (FEM) based on the theory of beam on elastic foundation using line element. The derived FEM was then applied to solve, for the first time, the pressure vessel problems with uniform thickness. Our FEM results, obtained even by using only one line element, agreed exactly with the available closed-form solution, confirming the validity and computing efficiency of our finite element formulation. Moreover, we have applied our new FEM to solve pressure vessel problems with non-uniform thickness where no exact analytical solution is known to exist. The distributions of discontinuity stress in the cylindrical part were obtained. We found that shear force and bending moment were indeed discontinuous at the geometrically discontinuous juncture, due to the bending rigidity and elastic constant change by the non-uniform thickness. Finally, the case of discontinuity stresses in a bimetallic joint was also studied. The locations of maximum shear force and bending moment were found to be affected by the bending rigidity of the material.

Keywords: FEM; Pressure vessel; Elastic foundation

1. Introduction

Secondary stresses are those stresses developed by constraint of adjacent parts or by self-constraint of a structure, and are self-limiting. All thermal stresses produced by thermal gradients within a structure are secondary in nature. Another source of secondary stresses in a pressure vessel is that occurring at the juncture of the cylindrical vessel and its closure head, due to the different growth or dilation of the parts under pressure [1, 2].

Since the radial displacement of a cylindrical vessel with uniform thickness subjected to symmetric loading can be considered as deflection of a longitudinal element of unit width, the element therefore acts as a beam on elastic foundation. The governing equations of beam on elastic foundation have been used to analyze problems in pressure vessels, and excellent results were obtained for symmetric cases with uniform thickness [3, 4]. However, for pressure vessels with non-uniform thickness or different material properties there exists no analytical solution. Recently, finite element method (FEM)

* Corresponding author.

0168-874X/98/$19.00
PII S0168-874X(97)00041-3

has been applied to solve objects with arbitrary geometries where analytical solutions are difficult, if not impossible, to obtain [5–9]. Among them, the asymmetric finite element using triangular element has been applied to pressure vessels with discontinuity stress [8, 9]. Since it is a two-dimensional problem, to save CPU computing time, beam element using two nodes with four degrees of freedom [8] has been applied to solve such problems. However, poor agreements were obtained. This is because the governing equation of beam on elastic foundation is quite different from the general beam on structure. The strain energy and elastic potential on the elastic foundation change according to the beam length and the structure stiffness. To achieve accurate results, large number of elements are normally required, resulting in significant CPU time. Moreover, if the beam length is not properly chosen, significant errors could occur. To alleviate the above short comings, we report in this paper, the development of a finite element formulation using the exact displacement as shape function. Line element with two nodes was used in this study. We demonstrate, for the first time, that our FEM can be applied very efficiently to solve problems with non-uniform thickness and different material properties. The error is found to be less than 0.01% for all the examples with existing analytical solution we studied, even for the one-element case. The CPU time is, in general, only a few second, confirming the validity and excellent computing efficiency of our FEM formulation.

2. Finite element formulation of beam on elastic foundation

The governing equation of beam on elastic foundation as shown in Fig. 1 has the form

$$EI\frac{\mathrm{d}^4 y}{\mathrm{d}x^4} = -ky. \tag{1}$$

The general solution is

$$y = \mathrm{e}^{\beta x}(c_1 \cos\beta x + c_2 \sin\beta x) + \mathrm{e}^{-\beta x}(c_3 \cos\beta x + c_4 \sin\beta x), \tag{2}$$

where

$$\beta = \left(\frac{k}{4EI}\right)^{1/4}.$$

The boundary conditions are:

$$\begin{aligned} y(0) &= U_{2i-1} = c_1 + c_2, \\ \frac{\mathrm{d}u}{\mathrm{d}x}(0) &= U_{2i} = \beta(c_1 + c_2 - c_3 + c_4), \end{aligned} \tag{3}$$

where U_{2i-1} is the nodal displacement.

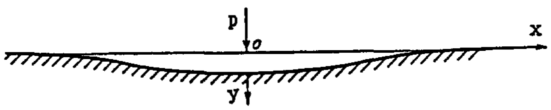

Fig. 1. Schematic of a beam on an elastic foundation.

By solving Eqs. (2) and (3), the coefficient can be obtained:

$$\begin{Bmatrix} c_1 \\ c_2 \\ c_3 \\ c_4 \end{Bmatrix} = \frac{1}{A_0} \begin{bmatrix} A_{11} & A_{12} & A_{13} & A_{14} \\ A_{21} & A_{22} & A_{23} & A_{24} \\ A_{31} & A_{32} & A_{33} & A_{34} \\ A_{41} & A_{42} & A_{43} & A_{44} \end{bmatrix} \begin{Bmatrix} U_{2i-1} \\ U_{2i} \\ U_{2j-1} \\ U_{2j} \end{Bmatrix}. \tag{4}$$

The elements of matrix are shown in Appendix A.

The displacements of element are:

$$u = N_{2i-1}U_{2i-1} + N_{2i}U_{2i} + N_{2j-1}U_{2j-1} + N_{2j}U_{2j}, \tag{5}$$

where N_{2i-1}, N_{2i}, N_{2j-1}, N_{2j} is the shape factor with the value

$$\begin{Bmatrix} N_{2i-1} \\ N_{2i} \\ N_{2j-1} \\ N_{2j} \end{Bmatrix} = [A]^{\mathrm{T}}\{\phi\}, \tag{6}$$

where

$$\{\phi\} = \begin{Bmatrix} \mathrm{e}^{\beta x}\cos\beta x \\ \mathrm{e}^{\beta x}\sin\beta x \\ \mathrm{e}^{-\beta x}\cos\beta x \\ \mathrm{e}^{-\beta x}\sin\beta x \end{Bmatrix}.$$

The strain energy of beam is

$$\Lambda^{(e)} = \frac{EI}{2}\int_0^L \left(\frac{\mathrm{d}^2u}{\mathrm{d}x^2}\right)^2 \mathrm{d}x = \frac{EI}{2}\{U\}^{\mathrm{T}}[A]^{\mathrm{T}}\frac{\beta^3}{2}[B^1][A]\{U\}. \tag{7}$$

The elements in $[B^1]$ is B^1_{ij}

$$B^1_{ij} = \int_0^L \frac{\mathrm{d}^2\phi_i}{\mathrm{d}x^2}\frac{\mathrm{d}^2\phi_j}{\mathrm{d}x^2}\,\mathrm{d}x = B^1_{ji}. \tag{8}$$

The potential energy by elastic support is

$$\Lambda^{(e)}_{\mathrm{e}} = \frac{1}{2}\int_0^L k u^2\,\mathrm{d}x = \tfrac{1}{2}k\{U\}^{\mathrm{T}}[A]^{\mathrm{T}}(1/8\beta)[B^2][A]\{U\}. \tag{9}$$

The elements of matrix $[B^2]$ are shown in Appendix B.

The total potential energy of element is

$$\Lambda^{(e)} = \tfrac{1}{4}EI\beta^3\{U\}^{\mathrm{T}}[A]^{\mathrm{T}}([B^1] + [B^2])[A]\{U\}. \tag{10}$$

Taking variation with respect to displacement, we get

$$[K^e] = \tfrac{1}{2}\beta^3[A]^{\mathrm{T}}([B^1] + [B^2])[A]. \tag{11}$$

The elements of matrix $[K^e]$ are shown in Appendix C.

3. Numerical examples and discussion

Example 1. To verify the derived finite element method, a single concentrated load acts on the left side of a beam on the elastic foundation, as shown in Fig. 2, is chosen as an example. The material properties are:

rigidity $EI = 10^4\,\mathrm{N\,m^2}$, spring constant $k = 25$ Mpa.

The numerical results using both one and two elements are obtained. The radial deflection, rotation angle, moment, and shear force in the x-direction are plotted in Figs. 3(a)–(d), respectively. The

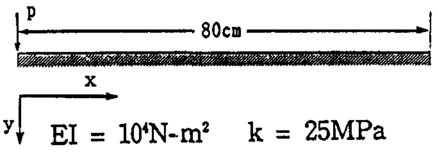

Fig. 2. A single concentrated load acts on the left side of a beam on an elastic foundation.

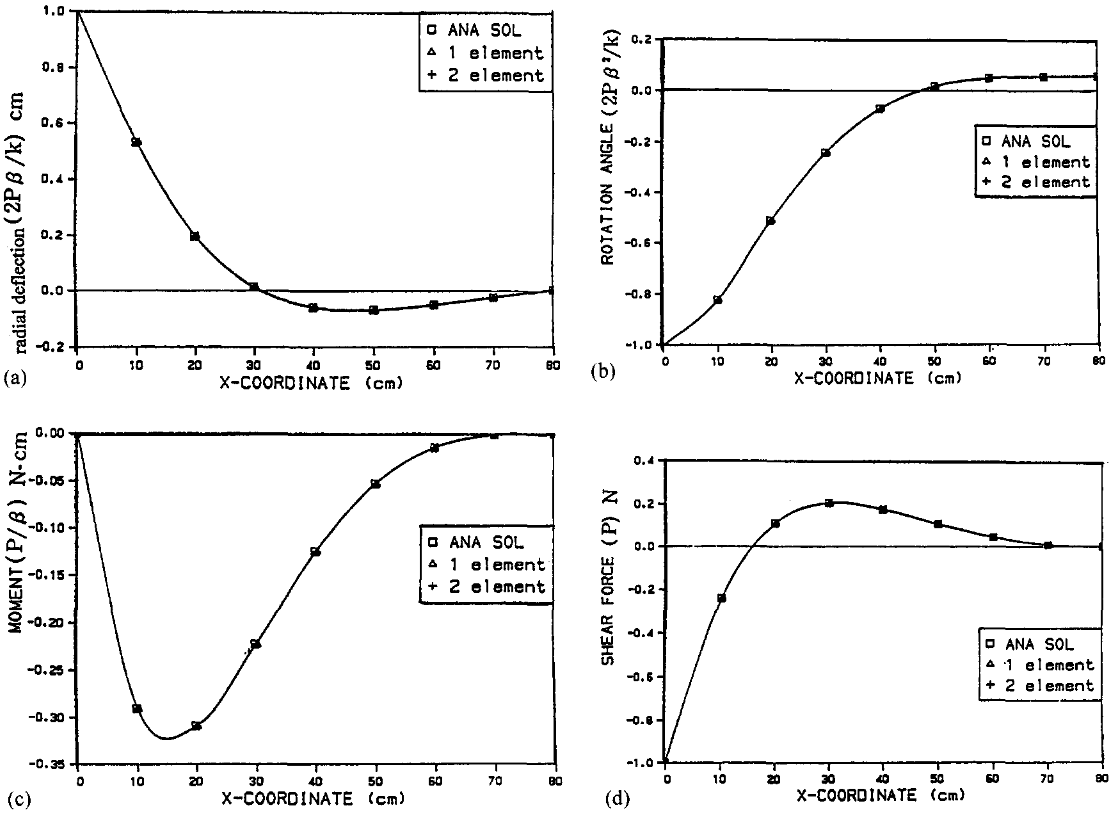

Fig. 3. Numerical results for a single concentrated load acting on the left side of a beam on an elastic foundation, using one element (triangle) and two element (+), and the corresponding analytical solutions [1] (square) for (a) the radial deflection in the x-direction, (b) the rotation angle in the x-direction, (c) the moment in the x-direction, and (d) the shear force in the x-direction.

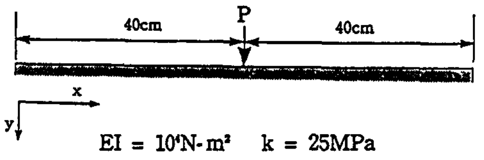

Fig. 4. A single concentrated load acts instead on the middle of a beam on an elastic foundation.

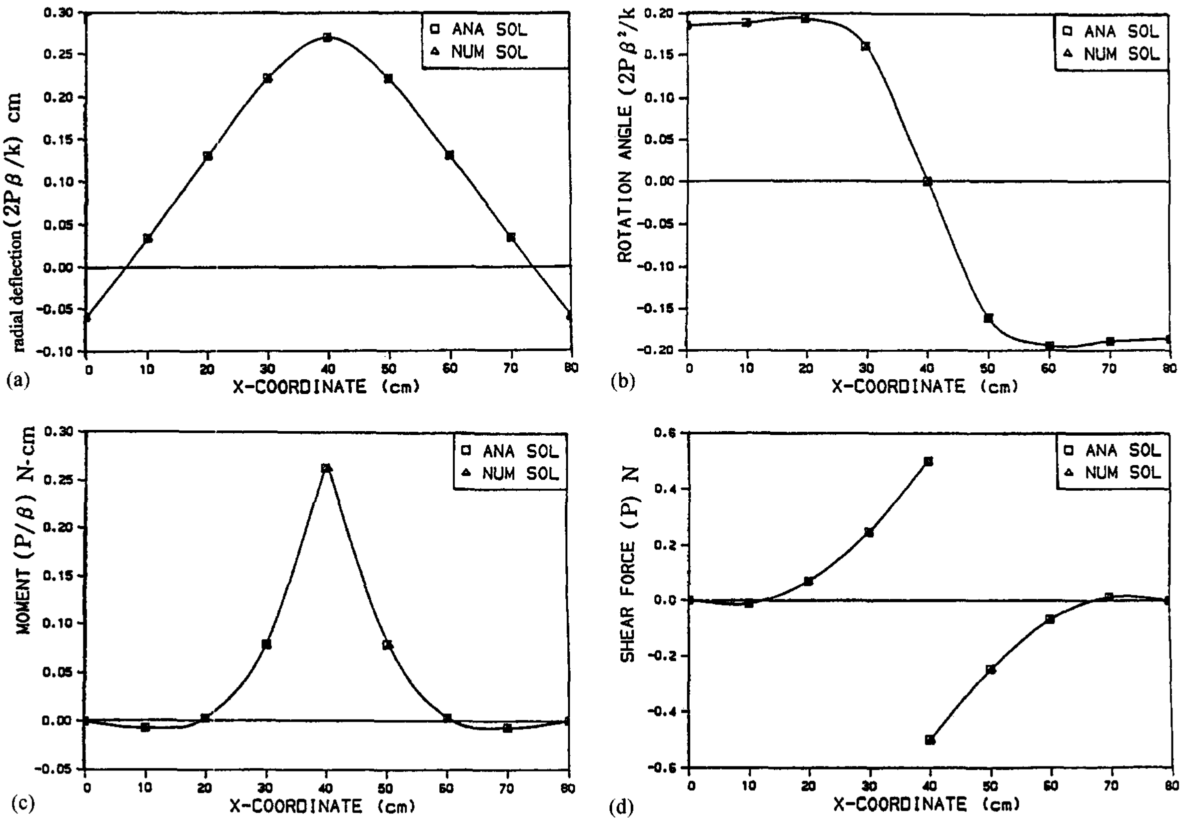

Fig. 5. Numerical results for a single concentrated load acting instead on the middle of a beam on an elastic foundation, together with the available analytical solution (square) for (a) the displacement in x-direction, (b) the rotation angle in x-direction, (c) the moment in x-direction, and (d) the shear force in x-direction.

corresponding analytical solutions from Ref. [4] are also plotted for comparison. Excellent agreements with the analytical solutions are obtained. The error is less than 0.01%, even for the one-element case, confirming the validity and excellent computing efficiency of our FEM formulation.

Example 2. A single concentrated load, identical to that used in the first example, acts instead on the middle of a beam on elastic foundation as shown in Fig. 4.

The numerical results from FEM formulation are again obtained by using both one and two elements. The displacement, rotation angle, moment, and shear force are plotted in Figs. 5(a)–(d), respectively, together with the corresponding analytical solutions available in the literature [2]. The

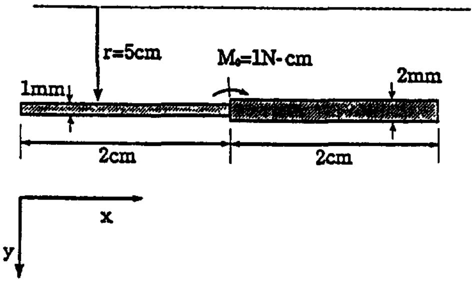

Fig. 6. A unit moment is acting on the middle point of a beam with non-uniform thickness.

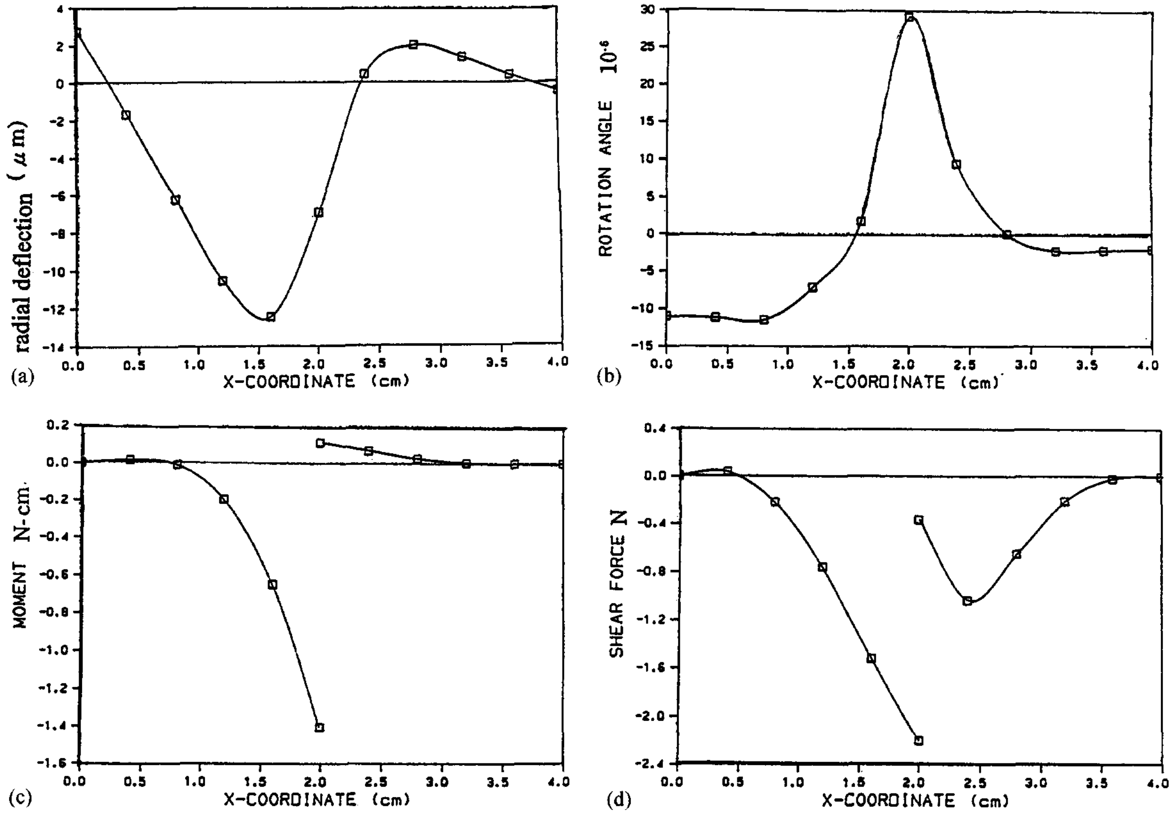

Fig. 7. Numerical results for a unit-moment acting on the middle point of a beam with non-uniform thickness for (a) displacement in the x-direction, (b) the rotation angle in x-direction, (c) the moment in x-direction, and (d) the shear force in x-direction.

error is less than 0.01%, even for the one-element case, confirming again that excellent agreements and computing efficiency are obtained.

Example 3. In this example, we apply our finite element formulation to solve, for the first time, problem with non-uniform thickness, where no exact solution is available. A tube with 5 mm in

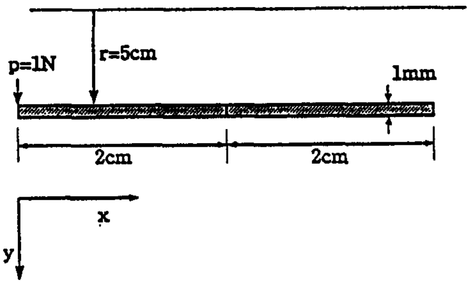

Fig. 8. A cylindrical pressure vessel with bimetallic joint.

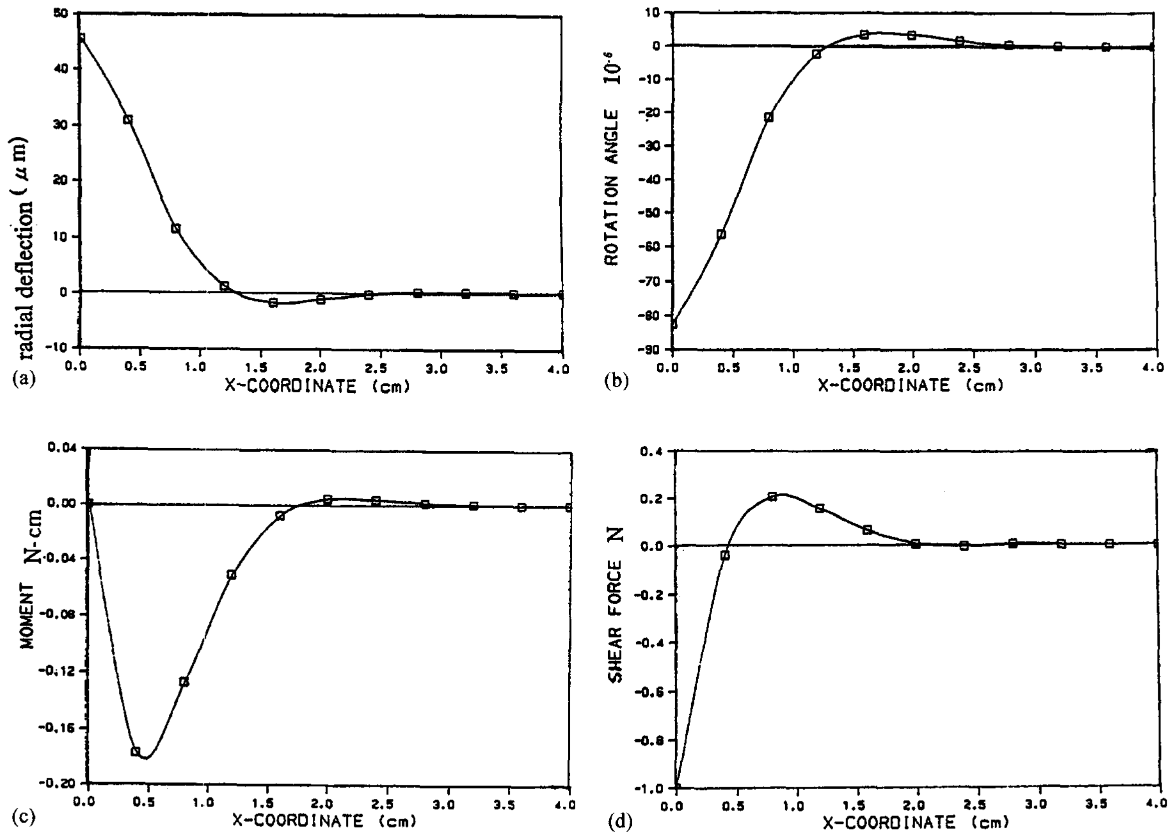

Fig. 9. Numerical results for a cylindrical pressure vessel with bimetallic joint for (a) the displacement in x-direction, (b) the rotation angle in x-direction, (c) the moment in x-direction, and (d) the shear force in x-direction.

radius, 0.3 in Poisson ratio, and Young's modulus of 20 GPa is chosen. The thickness of the left-hand side is 1 mm, while the thickness of the right-hand side is 2 mm, as shown in Fig. 6. A unit moment is assumed to be acting on the middle point of the beam.

The FEM results are shown in Figs. 7(a)–(d). The maximum deflection occurs on the left-hand side (i.e., thinner side) near the acting moment (Fig. 7(a)). The deflection is larger on the thinner side because its rigidity is smaller. The rotation angle of the thinner side is also larger than that of the thicker side (Fig. 7(b)). As shown in Fig. 7(c) and Fig. 7(d), the moment and shear force at both ends are zero, corresponding to the fact that there are no support at both ends. The results also show that the moment and shear force are not symmetric at the juncture. More importantly, they are discontinuous at the juncture as a result of the bending rigidity and elastic constant change due to the thickness of nonuniformity.

Example 4. In this example, we apply our FEM using two elements to solve, for the first time, problem with different materials, where no analytical solution exists. A cylindrical pressure vessel with bimetallic joint, as shown in Fig. 8, is chosen for this purpose. The radius is 5 cm and the thickness is 1 mm. The material constants are: Poisson's ratio = 0.3, Young's modulus for the left-hand side is 20 Gpa, Young's modulus for the right-hand side is 10 Gpa. The vessel is subjected to a concentrated load at the left-hand side.

The numerical results on the deflection distribution and rotation angle along the x-direction are shown in Figs. 9(a) and (b), respectively. The maximum displacement and rotation angle are found to occur at the point where the load is acted (i.e., left-hand side). As shown in Fig. 9(c), the moments at both ends are found to be zero, however, the vessel depicts a maximum moment near the point where the load is acted (i.e., 0.5 cm from the left-hand side). The shear force at the end of the right-hand side is zero, while its maximum occurs at the left-hand side, as shown in Fig. 9(d).

4. Conclusions

In this study, we have applied the variation principle and developed a finite-element formulation to solve beam on elastic foundation and cylindrical pressure vessel. We have verified the validity and efficiency of the newly developed FEM method by comparing the numerical results with existing analytical solutions for problems with uniform thickness. In addition, we have also applied the new FEM formulation to solve, for the first time, more general problems such as vessels with different thickness or different materials. We found that for the vessel with different materials, the moment and shear force are not symmetric and are actually discontinuous at the juncture as a result of the bending rigidity and elastic constant change. We also found that the vessel with non-uniform thickness depicts a maximum moment near the point where the load is acted. The shear force is at its maximum at the end where the load is acted, and approaches zero at the other end.

Appendix A

The elements for A_0 and A_{ij} in Eq. (4) are:

$$A_0 = 4\beta^2(\sinh^2 \beta L - \sin^2 \beta L),$$

$$A_{11} = \beta^2[e^{-2\beta L} - 1 - 2\sin^2 \beta L \cos \beta L],$$

$$A_{21} = \beta^2[e^{-2\beta L} + 1 - 2\cos^2 \beta L - 2\sin \beta L \cos \beta L],$$

$$A_{31} = \beta^2[e^{2\beta L} - 1 - 2\sin^2 \beta L + 2\sin \beta L \cos \beta L],$$

$A_{41} = \beta^2[\mathrm{e}^{2\beta L} + 1 - 2\cos^2\beta L + 2\sin\beta L\cos\beta L],$

$A_{12} = -2\beta\sin^2\beta L,$

$A_{22} = \beta[\mathrm{e}^{2\beta L} - 1 + 2\sin\beta L\cos\beta L],$

$A_{32} = 2\beta\sin^2\beta L,$

$A_{42} = \beta[\mathrm{e}^{2\beta L} - 1 - 2\sin\beta L\cos\beta L],$

$A_{13} = \beta^2[\mathrm{e}^{\beta L}(\cos\beta L + \sin\beta L) - \mathrm{e}^{-\beta L}(\cos\beta L - \sin\beta L)],$

$A_{23} = \beta^2[-\mathrm{e}^{\beta L}(\cos\beta L - \sin\beta L) + \mathrm{e}^{-\beta L}(\cos\beta L - 3\sin\beta L),$

$A_{33} = \beta^2[-\mathrm{e}^{\beta L}(\cos\beta L + \sin\beta L) + \mathrm{e}^{-\beta L}(\cos\beta L - \sin\beta L),$

$A_{43} = \beta^2[-\mathrm{e}^{\beta L}(\cos\beta L + 3\sin\beta L) + \mathrm{e}^{-\beta L}(\cos\beta L + \sin\beta L),$

$A_{14} = -\beta[\mathrm{e}^{\beta L}\sin\beta L - \mathrm{e}^{-\beta L}\sin\beta L],$

$A_{24} = \beta[\mathrm{e}^{\beta L}\cos\beta L - \mathrm{e}^{-\beta L}(\cos\beta L + 2\sin\beta L),$

$A_{34} = \beta[\mathrm{e}^{\beta L}\sin\beta L - \mathrm{e}^{-\beta L}\sin\beta L],$

$A_{44} = \beta[\mathrm{e}^{\beta L}(2\sin\beta L - \cos\beta L) + \mathrm{e}^{-\beta L}\cos\beta L.$

Appendix B

In Eq. (9), $[B^2]$ is a symmetry matrix, the elements are:

$B^2_{11} = \mathrm{e}^{2\beta L}[1 + 2\cos^2\beta L + 2\sin\beta L\cos\beta L) - 3,$

$B^2_{12} = 1 - \mathrm{e}^{2\beta L}[1 - 2\sin^2\beta L - 2\sin\beta L\cos\beta L],$

$B^2_{13} = 4\beta L + 4\sin\beta L\cos\beta L,$

$B^2_{14} = 4\sin^2\beta L,$

$B^2_{22} = \mathrm{e}^{2\beta L}[1 + 2\sin^2\beta L - 2\sin\beta L\cos\beta L] - 1,$

$B^2_{23} = 4\sin^2\beta L,$

$B^2_{24} = 4\beta L - 4\sin\beta L\cos\beta L,$

$B^2_{33} = 3 - \mathrm{e}^{-2\beta L}[1 + 2\cos^2\beta L - 2\sin\beta L\cos\beta L),$

$B^2_{34} = 1 - \mathrm{e}^{-2\beta L}[1 - 2\sin^2\beta L + 2\sin\beta L\cos\beta L),$

$B^2_{44} = 1 - \mathrm{e}^{-2\beta L}[1 + 2\sin^2\beta L + 2\sin\beta L\cos\beta L).$

Appendix C

In Eq. (11) $[K^e]$ is a symmetry matrix, and the elements are:

$$K_{11}^e = 2H\beta^2(\sinh\beta L\cosh\beta L + \sin\beta L\cos\beta L),$$

$$K_{12}^e = H\beta(\sinh^2\beta L + \sin^2\beta L),$$

$$K_{13}^e = -2H\beta^2(\sin\beta L\cosh\beta L + \sinh\beta L\cos\beta L),$$

$$K_{14}^e = 2H\beta\sinh\beta L\sin\beta L,$$

$$K_{22}^e = H(\sinh\beta L\cosh\beta L - \sin\beta L\cos\beta L)$$

$$K_{23}^e = -K_{14}^e$$

$$K_{24}^e = H(\sin\beta L\cosh\beta L - \sinh\beta L\cos\beta L)$$

$$K_{33}^e = K_{11}^e$$

$$K_{34}^e = K_{12}^e$$

$$K_{44}^e = K_{22}^e$$

where

$$H = \frac{2EI}{\sinh^2\beta L - \sin^2\beta L}.$$

References

[1] G.W. Watts, H.A. Lang, Stresses in a pressure vessel with a conical head, ASME Transactions Paper 51-PET-8, April 1952.

[2] W.J. Graff, Junction stresses for a conical section joining cylinders of different diameter subject to internal pressure, ASME Publication Paper No. 76-PET-31, 1976.

[3] J.F. Harvey, Pressure Component Construction, Reinhold Company, Van Nostrand, 1980.

[4] M. Hetenyi, Beams on Elastic Foundation, The University of Michigan Press, Ann Arbor, 1979.

[5] F.Y. Huang, K.Z. Liang, Torsional analysis of micropolar elasticity using the finite element method, Internat. J. Eng. Sci. 32 (2) (1994) 347–358.

[6] F.Y. Huang, K.Z. Liang, Boundary element for micropolar thermoelasticity, Eng. Anal. Boundary Element 17 (1996) 19–26.

[7] K.Z. Liang, F.Y. Huang, Boundary element for micropolar elasticity, Internat. J. Eng. Sci. 34 (5) (1996) 509–521.

[8] T.R. Chandrupatla, A.D. Belegundu, Introduction to Finite Elements in Engineering, Prentice-Hall, Englewood Cliffs, NJ, 1991.

[9] L.J. Segerlind, Applied Finite Element Analysis, 2nd ed., Wiley, New York, 1984.